Designing localized multipulse solutions of the discrete nonlinear Schrödinger equation with an external potential

D. Hennig and H. Gabriel
Freie-Universität-Berlin, Fachbereich Physik, Institut für Theoretische Physik Arnimallee 14, 14195 Berlin, Germany
(Received 20 August 1997)

We construct standing localized multipulse states for the nonintegrable discrete nonlinear Schrödinger equation (DNLS) with an external potential. The construction method is based on a nonlinear map approach, the orbits of which represent stationary solutions of the DNLS. The single (stationary) soliton states of the DNLS lattice are associated with single-pulse homoclinic and heteroclinic connections. It is demonstrated that the external potential can be adopted to excite multiple solitons at arbitrarily chosen locations on the lattice. Furthermore, multiple soliton states having different maximal amplitudes are excited. Finally, we use the orbits of the stationary map as initial conditions to design stationary localized multipulse solutions in the dynamics of the (time-dependent) discrete nonlinear Schrödinger equation and discuss their linear stability. [S1063-651X(98)06802-0]

PACS number(s): 03.40.Kf, 63.20.Pw, 63.20.Ry

I. INTRODUCTION

The nonlinear Schrödinger equation (DNLS) represents a prototype of a nonlinear lattice system that consists of coupled nonlinear oscillators. The physical relevance of the DNLS is documented in a series of publications [1–8]. A typical feature described by the DNLS is the ability of self-trapping of certain physical quantities (e.g., excitation energy) as intrinsic localized modes at a single site or a few sites of the lattice.

For illustration we quote here the application of DNLS in optics when it models the propagation of electromagnetic waves in arrays of coupled nonlinear optical waveguides [9–13]. A key problem in the study of the DNLS (not only in the optical context) is the determination of the stable localized excitation modes, which can serve for the reliable storage of energy [14–19,11]. The discrete intrinsic localized modes of nonlinear lattices have attracted recently much interest and rigorous results concerning their existence and stability have been derived [20,21]. Recently, such localized modes have been experimentally observed in an electrical network also modeled by a DNLS [22].

For integrable continuous systems (partial differential equations), such as the continuum nonlinear Schrödinger equation (NLS), well-developed methods exist to construct soliton solutions. These solitons accomplish optimal lossless energy storage and energy transport, respectively [23]. However, the discrete version of the NLS in the form used in many applications [see Eq. (1) below] is nonintegrable [24,25] and therefore do not exhibit exact soliton solutions. Nevertheless, as demonstrated in [26] the excitation of stable localized single-pulse states of the DNLS is possible despite its nonintegrability property. It is shown in detail that the results of a stationary analysis can be used to excite localized stationary states of designed amplitude and pulse width on the lattice. The stationary DNLS problem can be tackled by a nonlinear map approach (for details we refer to [26]). It is demonstrated that stable localized lattice states are supported by map orbits related to homoclinic and heteroclinic connections. These homoclinic and heteroclinic orbits deliver the single-pulse localized states on the lattice in the form of dark and bright solitons. However, with view to application it is desirable that the lattice supports also solutions with multiple pulses carrying the energy in several portions.

The present paper is devoted to constructing such multiple soliton states for the DNLS with an external potential. The method is based on a repeated use of the same single-pulse homoclinic (heteroclinic) map orbit for suitable iteration intervals of the nonlinear map. To this aim we adopt the external potential such that the homoclinic orbit is left at a homoclinic point near the hyperbolic equilibrium to be continued as a linear periodic orbit of tiny amplitude for a selected iteration interval (lattice section). Eventually, the homoclinic orbit is reentered to excite another soliton pulse on the lattice.

The current approach differs from the treatment of multiple-pulse orbits based on the complicated properties of a homoclinic tangle associated with a nonintegrable map (or Poincaré surfaces of sections of chaotic time-dependent systems). A single-pulse homoclinic (heteroclinic) orbit makes on excursion away from some hyperbolic equilibrium point (or a periodic orbit, or invariant torus), and then returns to it for an infinite number of iterations (in infinite time in the case of time-dependent systems). Moreover, there exists also other types of homoclinic orbits that make more than one excursion away from the hyperbolic equilibrium point. The result is a multiple pulse homoclinic orbit [27–30]. However, this process reveals a complicated irregular spatial (and/or temporal) jumping behavior between subsequent pulses. Multiple-pulse jumping orbits have been discussed, e.g., in the context of a modal truncation (two modes) of the damped-forced NLS [31–33] and also in [34,35]. We underline that the advantage of our method of constructing multipulse solutions based on regaining the same single-pulse homoclinic (heteroclinic) orbit is that we not only *control* the spatial distance between consecutive pulses, but are also able to tailor the amplitudes of the pulses, individually.

The paper is organized as follows: In Sec. II we describe the DNLS equation with external potential. The stationary DNLS problem is introduced and attributed to a two-dimensional nonlinear map. In Sec. III we present the methods for constructing multiple soliton solutions at selected

lattice locations and/or of selected amplitudes. These stationary multiple soliton states are then used as initial conditions for the time-dependent DNLS to create standing localized solutions showing multiple pulses. Finally, we discuss the stability properties of the localized multipulse excitations.

II. THE DISCRETE NONLINEAR SCHRÖDINGER EQUATION

We study the discrete nonlinear Schrödinger equation (DNLS)

$$i\frac{d\psi_n(t)}{dt} = -\gamma|\psi_n(t)|^2\psi_n(t) - V[\psi_{n+1}(t)+\psi_{n-1}(t)] - F_n\psi_n(t), \tag{1}$$

where $\psi_n(t)$ is a complex amplitude, γ is the nonlinearity strength, and V is the transfer matrix element coupling adjacent oscillators at lattice sites n and $n\pm1$, respectively. F_n determines a static external potential (field) with real-valued amplitudes along the lattice. The dynamics of nonlinear Schrödinger equations (including the integrable Ablowitz-Ladik equation) with external spatially uniform and time-varying potentials $F_n(t)=\mathcal{E}(t)n$ has been studied in [24,36,37]. These studies focused mainly on the integrability and the existence of both soliton and breather solutions as well as a dynamically induced localization in the presence of the field.

We are interested in time-periodic, but spatially localized solutions of Eq. (1). Substituting the ansatz

$$\psi_n(t)=\phi_n\exp(-i\omega t), \tag{2}$$

with real amplitudes ϕ_n and the phase (oscillation frequency) ω into Eq. (1), we derive the following two-dimensional map $R^2\to R^2$ by defining $x_n=\phi_n$ and $y_n=\phi_{n-1}$ where the lattice index plays the role of a discrete ''time''

$$\mathcal{M}:\begin{cases} x_{n+1}=-(\omega+\gamma x_n^2+F_n)x_n/V-y_n \\ y_{n+1}=x_n \end{cases}. \tag{3}$$

This map has been studied in the free-field case $F_n=0$ in [6,38,39,26].

For practical reasons lattice chains of large but finite number N of sites of order 200 are chosen. The map $\mathcal{M}$ is initiated with a starting value $(x_1,y_1)\equiv(\phi_1,\phi_0)$ corresponding to the first two lattice amplitudes at the left end of the chain. With each iteration step we gain then the amplitude at the lattice next towards the right end of the chain.

For later use we briefly review the properties of the map $\mathcal{M}$ in the free-field case of $F_n=0$ [26]. Reversibility of the map $\mathcal{M}$ is established by the factorization $\mathcal{M}=\mathcal{M}_0\mathcal{M}_1$ with

$$\mathcal{M}_0:\begin{cases} x_{n+1}=y_n \\ y_{n+1}=x_n \end{cases} \tag{4}$$

and

$$\mathcal{M}_1:\begin{cases} x_{n+1}=x_n \\ y=-(\omega+\gamma x^2)\,x_n/V-y_n, \end{cases} \tag{5}$$

where $\mathcal{M}_{0,1}$ are involutions and their corresponding symmetry lines are given by S_0: $x=y$ and S_1: $y=-(1/2)(\omega x+\gamma x^3)/V$. The inverse map is determined by $\mathcal{M}^{-1}=\mathcal{M}_1\mathcal{M}_0$.

To obtain stationary localized solutions in the form of bright (dark) solitons, it suffices to study the fixed points (period-1 orbits) of the map $\mathcal{M}$ [26], which are located at

$$\hat{x}_0=0, \quad \hat{x}_\pm=\pm\sqrt{-\frac{\omega+2V}{\gamma}}, \tag{6}$$

where $\hat{x}_\pm$ exists only if $\mathrm{sgn}(\omega+2V)=-\mathrm{sgn}(\gamma)$.

The results of the stability analysis of the fixed point $(\hat{x}_0,\hat{y}_0)$ at the origin can be summarized as follows [26]:

Case	ω/V	$\mathrm{sgn}(\gamma)$	Stability
(i)	$>-2,<2$	>0	elliptic
(ii)	$>-2,<2$	<0	elliptic
(iii)	<-2	>0	hyperbolic
(iv)	>2	<0	reflection hyperbolic

Concerning the pair of points $(\hat{x}_\pm,\hat{y}_\pm)$ their stability properties are given by

Case	Stability
(ii)	hyperbolic
(iii)	elliptic
(iv)	elliptic

Since the map $\mathcal{M}$ is nonintegrable [26], the stable and unstable manifolds belonging to the unstable hyperbolic fixed points intersect each other transversely yielding homoclinic orbits to the point $(\hat{x}_0,\hat{y}_0)$ in the cases (iii) and (iv) whereas in case (ii) heteroclinic orbits connecting the points $(\hat{x}_+,\hat{y}_+)$ and $(\hat{x}_-,\hat{y}_-)$ result.

We described in [26] how the homoclinic and heteroclinic orbits of the map $\mathcal{M}$ support single-pulse localized solutions on the DNLS lattice. In case (iii) there exist two homoclinic orbits whose points alternate along the invariant manifolds. Each of the homoclinic orbits has one of its points on the symmetry line S_0 and S_1, respectively. Under the mapping these points rapidly approach the map plane origin. The homoclinic orbit crossing S_0, which we denote by $\{\phi_{\mathrm{even}}\}$, represents a stationary excitation pattern $(\cdots\uparrow\uparrow\uparrow\uparrow\cdots)$ on the lattice chain, called even-parity mode in [40] and sometimes also intersite centered local mode [19]. (The dots stand for vanishingly small amplitudes in the exponential tail of the excitation pattern.) The other homoclinic orbit $\{\phi_{\mathrm{odd}}\}$ has one member on S_1 and obeys the mode pattern $(\cdots\uparrow\uparrow\uparrow\cdots)$ with three large amplitudes called odd-parity mode [41] or on-site centered local mode [19].

In case (iv) the homoclinic map orbit supports a soliton-like solution on the lattice chain which exists in the gap

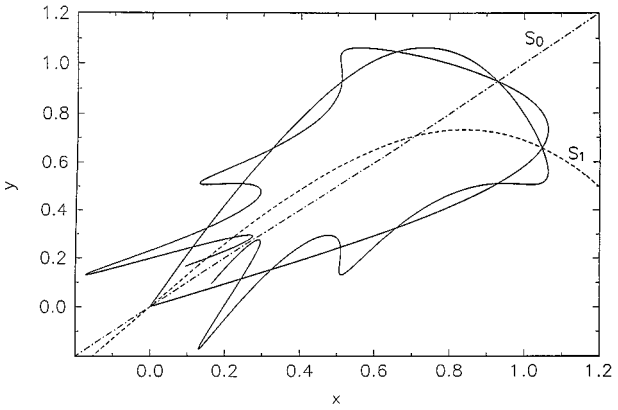

FIG. 1. First windings of the homoclinic tangle of the hyperbolic equilibrium point at (0,0) for the map $\mathcal{M}$ in the free-field case $F_n=0$. The symmetry lines S_0 and S_1 are superimposed. Parameters: $\omega=-2.1$, $\gamma=1$, and $V=0.8$.

above the linear passing band ($\omega>2V$) and has alternating signs for adjacent amplitudes, i.e., $\mathrm{sgn}(\phi_{n+1})=-\mathrm{sgn}(\phi_n)$ as a characteristic feature. This stationary localized structure has been called a *staggered soliton* by Cai, Bishop, and Grønbech-Jensen in their study of the combined AL-DNLS equation [17]. Correspondingly, the soliton solution of case (iii) is called unstaggered soliton. Note that upon sign change $\gamma\rightarrow-\gamma$ and $\omega\rightarrow-\omega$, the map has the symmetry property $\mathrm{sgn}(\phi_{n+1})=-\mathrm{sgn}(\phi_n)$ so that the unstaggered and staggered soliton replace one another. For positive (negative) γ the unstaggered odd-parity (staggered even-parity) mode has lower energy than the unstaggered even-parity (staggered odd-parity) mode [17,26].

Concerning case (ii) the resulting heteroclinic map orbit represents a kinklike solution, also called a *dark soliton* on the lattice. There exist staggered and unstaggered versions of this soliton too.

In Fig. 1 we show the first windings of the stable and unstable manifolds of the hyperbolic fixed point at the origin in the x-y-map plane for case (iii). One clearly recognizes the homoclinic points as the intersection of the stable and unstable manifolds. We superimposed the symmetry lines S_0 and S_1. Taking the stationary odd-parity mode $\{\phi_{\mathrm{odd}}\}$ as the initial conditions $\psi_n(t=0)=\phi_n$ for the time-dependent system (1) the amplitude profile $|\psi_n(t)|^2$ of the standing bright solitonlike solution on the DNLS lattice is excited as depicted in Fig. 2. In Fig. 3 the even-parity localized mode is

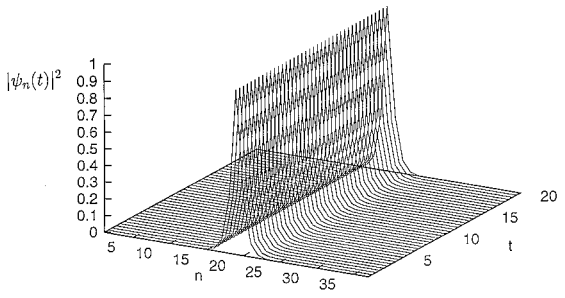

FIG. 2. The amplitude profile $|\psi_n(t)|^2$ showing the standing bright solitonlike solution on the DNLS lattice. The stationary soliton (odd-parity mode) is excited with the help of the homoclinic orbit with one point on S_1 on the map plane shown in Fig. 1.

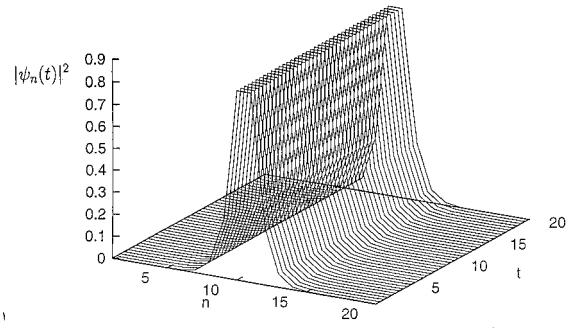

FIG. 3. The amplitude profile $|\psi_n(t)|^2$ of the even-parity localized mode.

shown. Note that for the excitation profile $|\psi_n(t)|^2$ the staggering of the amplitudes ϕ_n plays no role.

III. EXCITATION OF MULTIPULSE LOCALIZED STATES

We now turn to the map properties in the presence of the external field. It is a characteristic feature that the bright and dark solitonlike solutions of the DNLS in the free-field case represent single soliton excitations, i.e., their excitation patterns exhibit a single pulse (around the soliton center) of high (low) lattice amplitudes, which emerges from the background. On either side of the soliton center the amplitudes drop (rise) exponentially with increasing distance from the soliton center to vanishing amplitudes for the bright soliton (to a nonzero constant level for the dark soliton). In this section we show that for the DNLS with external potential F_n the excitation of multipulse localized states is possible.

We have just shown that for given sign of γ the existence as well as the type of solitonlike solutions depend on the value of the ratio ω/V. From Eq. (3) we infer immediately that the frequency ω can be tuned locally by the external potential F_n. In this way it is possible to ''jump'' at a certain iteration step of $\mathcal{M}$ deliberately from one orbit on the map plane of a given ω to different target orbits on the map planes belonging to $\tilde{\omega}_n=\omega+F_n$. Considering, for example, the potential

$$F_{n\geqslant 1}=-(\omega+\gamma\, x_1^2)-V\,(1+y_1/x_1)\ , \tag{7}$$

we obtain the linear map

$$\mathcal{M}_{\mathrm{lin}}:\begin{cases} x_{n+1}=y_n \\ \\ y_{n+1}=x_n\ , \end{cases} \tag{8}$$

giving orbits of period-1, that is a constant excitation pattern. Moreover, suppose one knows at the iteration ''time'' (lattice site) $m>1$ the coordinates (x_m,y_m) of one orbit member of an arbitrary (nonlinear) orbit, then this orbit can be left at that iteration ''time'' m to proceed as a linear period-1 orbit $x_{j+1}=x_j$ by adapting the potential due to Eq. (7) for $j\geqslant m$. After any iteration step the nonlinear map can be restored by switching off the external potential and hence the orbit is brought back to the original nonlinear one.

Multiple solitons at selected lattice sites

With respect to bright multiple solitonlike solutions of the DNLS, we can apply the method described above to create exact standing (single) soliton states at selected lattice locations. All we need is the knowledge of one member of the homoclinic orbit to a given set of parameters (ω,γ,V). This can be achieved via the normal form computation as described in [26]. The complete homoclinic orbit and hence the soliton state can be derived by iterating the map $\mathcal{M}$. The width of the soliton pulse that is governed by the dropoff of the amplitudes with increasing distance from the soliton center site m can be estimated by $|\phi_{m+k}| \leqslant \lambda^m |\phi_k|$ with $\lambda = [-\omega + \sqrt{\omega^2 - 4V^2}]/(2V)$ being the largest eigenvalue of the tangent map due to linearizing around the hyperbolic point. Note that the larger the ratio ω/V, i.e., the deeper ω lies in the gap below the linear passing band, the more rapid is the amplitude decay.

In order to excite well distinguished multipulse excitations on the lattice, we need to know beyond which lattice site the soliton amplitude has decayed sufficiently strong into the exponential tail of the soliton where the amplitudes are actually negligible. Then the orbit can be continued as a linear orbit of very small (constant) amplitudes for a selected iteration interval (lattice segment). Afterwards the orbit is forced back to a map plane on which it comes to lie on a homoclinic point departing from the origin with further map iterations and thus exciting another soliton pulse on the lattice. Therefore it is appropriate to define the *cutoff sites* as the lattice sites $m \pm k$ apart from the soliton center m such that $|\phi_{m\pm k}/\phi_m| \leqslant \epsilon \ll 1$. Since the homoclinic points approach the map origin asymptotically, the value of ϵ can be chosen arbitrarily small by selecting sufficiently the number n_ϵ of map iterations such that

$$n_\epsilon \geqslant \lambda^{-1} \epsilon^{1/m} . \tag{9}$$

(Very small amplitudes are typically obtained after $10-20$ iterations of the central soliton amplitude.)

The process of multisoliton creation proceeds in the following way: Firstly, we excite a single soliton centered around the site m_1 in the standard manner using the homoclinic orbit. At its cutoff site m_1+k_1 the external potential $F_{m_1+k_1} = -[\omega + \gamma(x_{k_1+m_1})^2] - V(1 + y_{k_1+m_1}/x_{k_1+m_1})$ is switched on to leave the homoclinic orbit and to enter the linear period-1 state of almost negligible amplitudes $x_j \equiv x_{k_1+m_1}$. After progressing a chosen number M of period-1 cycles the external potential can be switched off. To create the next lattice soliton centered at site k_1+m_1+M+1, the homoclinic orbit has to be reentered at the point $(y_{k_1+m_1}, x_{k_1+m_1})$, which amounts to a reverse operation of the last member of the linear period-1 orbit according to $(x_{k_1+m_1+M}, y_{k_1+m_1+M}) \rightarrow (y_{k_1+m_1+M}, x_{k_1+m_1+M})$. The reverse operation is described below [see Eq. (10)].

In this way we are able to excite multisoliton states having their soliton center at any selected lattice location. This is due to the switching mechanism *k_1 cycle of the linear period-1 orbit $\rightarrow$ homoclinic orbit $\rightarrow$ k_2 cycle of the linear period-1 orbit*, etc.

This process is illustrated in Fig. 4 for a two-soliton state. We computed the central (maximal) amplitude

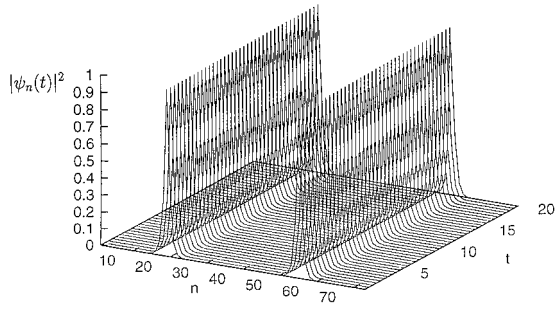

FIG. 4. A two-pulse solitonlike state (for details see text).

$\phi_c = 1.045\,789\,20$ of the soliton as the x coordinate of the homoclinic point (x_c^h, y_c^h) lying on the symmetry line S_1 for the parameters $\omega = -2.1$, $\gamma = 1$, and $V = 0.8$ analytically via the corresponding Birkhoff normal form [26]. With this starting value the map has been iterated to create a soliton on the lattice centered around the site $n = 19$. Since the soliton amplitudes at sites $n \geqslant 38$ fall below 10^{-5}, giving a ratio $\phi_{n\geqslant 38}/\phi_{19} < 2 \times 10^{-5}$, the site $n = 38$ has been taken to be the cutoff site. Here the external potential in the map is switched on appropriately to progress the period-1 orbit of very small amplitudes for eight cycles. Afterwards for $n \geqslant 49$ the orbit is traced back to the homoclinic orbit, which excites the second pulse of the two soliton state. Finally, we use the amplitude profile ϕ_n of the stationary two-soliton constructed with the help of the map $\mathcal{M}$ as the initial conditions for the time-dependent DNLS (1) with external potential to excite the standing two-soliton state shown in Fig. 4.

Strongly confined multisolitons of selected amplitudes

We now exploit the reversibility property of the map $\mathcal{M}$ to pass repeatedly through the single-pulse homoclinic orbit and excite *strongly confined multisoliton states*. To this aim we use the reflection symmetry of the map $\mathcal{M}$ on the line S_0. This means that for every homoclinic point (x^h, y^h) lying below the line $y = x$ for which $\phi_{k-1} < \phi_k$ there exists a mirror point (y^h, x^h) above that line with $\phi_{k-1} > \phi_k$. Under the action of the map $\mathcal{M}$ the amplitudes $(\phi_{k+1}, \phi_k) = \mathcal{M}(\phi_k, \phi_{k-1})$ grow (fall) for homoclinic points below (above) the line S_0, i.e., $|\phi_{k+1}| > |\phi_k|$ ($|\phi_{k+1}| < |\phi_k|$). In order to produce strongly confined multisolitons, we first excite a soliton using the homoclinic orbit. One takes a homoclinic point (x_k^h, y_k^h) below the line S_0 sufficiently close to the origin, such that the corresponding lattice amplitudes (ϕ_{k+1}, ϕ_k) (in the exponential tail of the soliton) are lower than the one at the cutoff site. The map $\mathcal{M}$ is iterated and eventually the homoclinic point (x_c^h, y_c^h) lying on the symmetry line S_1 is reached. The x coordinate of this point determines the maximum soliton amplitude ϕ_c. For further iteration the map orbit proceeds above the line S_0 until the corresponding mirror point (y_k^h, x_k^h) to the starting point (x_k^h, y_k^h) in the very vicinity of the map origin is reached. This yields a first soliton. Then we reverse the coordinates of the homoclinic point $(y_k^h, x_k^h) \rightarrow (x_k^h, y_k^h)$ with the following *reverse operation*:

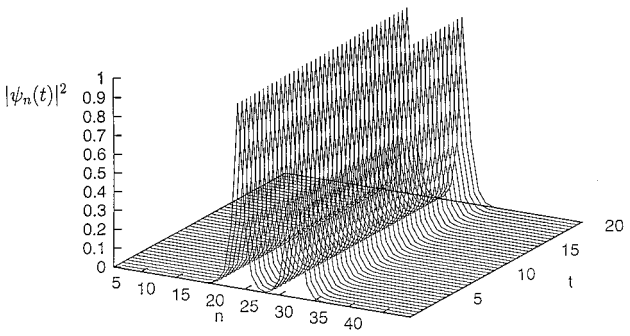

FIG. 5. Two very confined solitonlike states.

$$x_{k+1} = -(\omega + \gamma x_k^2 + F_k)x_k/V - y_k := y_k,$$

$$y_{k+1} = x_k, \tag{10}$$

which is accomplished by the local potential

$$F_k = -\left(\omega + \gamma x_k^2 + 2V\frac{y_k}{x_k}\right). \tag{11}$$

Therefore the map repeats the homoclinic orbit and a second soliton adjacent to the first is built up. Figure 5 shows such a two-soliton state for which one soliton is immediately followed by a second one.

The reverse operation can also be applied before the iteration of the starting point (x_k^h, y_k^h) reaches the homoclinic point (x_c^h, y_c^h) on S_1. In this fashion a soliton of amplitude less than the largest possible is excited. In dependence on the number n of iterations performed on the homoclinic orbit below S_0 before the reverse operation the resulting lattice soliton has a different maximal amplitude, that is, the larger n the higher the amplitude $\phi_{n+1} \leqslant \phi_c$.

In Fig. 6 we show a DNLS lattice exhibiting five solitons, the centers of which are positioned 31 lattice sites apart from each other. In creating this multipulse lattice excitation we applied both the method of creating solitons at chosen locations (see above) as well as the reverse operation to excite solitons of chosen amplitude.

The central soliton placed around the site $n = 81$ has the maximal possible amplitude ϕ_c determined by the x coordinate of the homoclinic point on S_1. The maxima of the two adjacent solitons to its left and right side correspond to the x coordinates of the homoclinic points preceding the point on S_1, respectively. Since the individual maxima of each soliton correspond to consecutive homoclinic points from the same

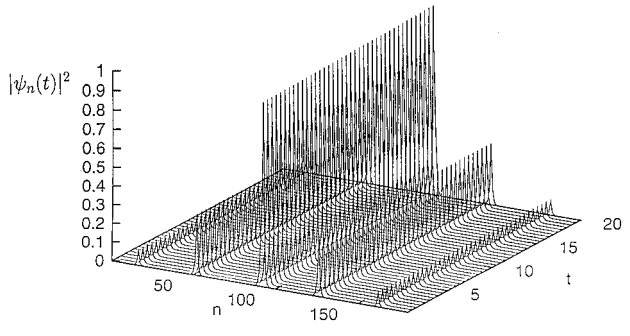

FIG. 6. A five-pulse lattice excitation.

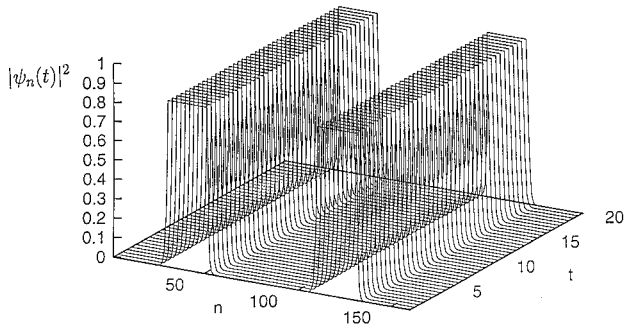

FIG. 7. A two-pulse state based on two even-parity localized modes with their maximal amplitudes continued over 20 lattice sites.

homoclinic orbit, the soliton maxima drop exponentially with increasing distance from the central soliton.

Solitons with more than two equal center amplitudes

Finally we demonstrate how solitons with more than two equal central sites can be excited. We recall that the two-site center of the staggered even-parity mode corresponds to a homoclinic point with $x_c^h = -y_c^h$. The two members $(\hat{x}_+, \hat{y}_-)$ and $(\hat{x}_-, \hat{y}_+)$ of the period-2 orbit exhibit the same symmetry. Therefore, the even-parity center can be continued over more than two lattice sites as a period-2 orbit by applying the following external potential, which turns the soliton center into a period-2 orbit [cf. Eq. (6)]

$$F = -[\omega + 2V + (x_c^h)^2]. \tag{12}$$

Combining this method of continuing a period-2 orbit with the technique of switching from a linear periodic orbit to the homoclinic orbit (and vice versa), we create the excitation pattern shown in Fig. 7. The even-parity center amplitudes have been kept for 20 lattice sites for each of the two solitons.

IV. LINEAR STABILITY

We have used the map orbits of the different stationary multipulse excitations as initial conditions for the time-dependent DNLS (1) with external potential to excite standing multisoliton solutions. This proceeds in the same way as in [26] to excite single soliton states for the free-field DNLS. An important question is whether these stationary states $\psi_n(t) = \phi \exp(-i\omega t)$ are linearly stable. For perturbations $u_n(t)$ of the stationary solutions maintaining the symmetry properties of the excitation pattern, (e.g., for the unstaggered solitons with real $\phi_n \geqslant 0$ all u_n must be real and nonnegative) we can construct a Lyapunov function assuring stability. We exploit the conserved quantity $P = \Sigma_n |\psi_n|^2$. As the Lyapunov function we take

$$L = P - P_s, \tag{13}$$

where $P_s = \Sigma_n \phi_n^2$. It is readily seen that

$$\frac{dL}{dt} = 0, \quad L(\phi_n) = 0, \quad L(\phi_n + u_n) \geqslant 0. \tag{14}$$

To investigate linear stability for arbitrary complex perturbations $u_n(t)$ we make the ansatz [1]

$$\psi_n(t)=[\phi_n+u_n(t)]\exp(-i\omega t)\ , \tag{15}$$

where $u_n(t)$ are small perturbations. Linearizing Eq. (1) we obtain the system in tangent space

$$i\frac{du_n}{dt}=-\gamma\ (2\phi_n^2u_n+\phi_n^2u_n^*)-V(u_{n+1}+u_{n-1}) -(\omega+F_n)u_n\ . \tag{16}$$

Setting $u_n=x_n+iy_n$ with real x and y and decomposing Eq. (16) into real and imaginary parts we obtain the system

$$\dot{x}=-(\gamma\phi_n^2+\omega+F_n)\ y_n-V(y_{n+1}+y_{n-1}), \tag{17}$$

$$\dot{y}=(3\gamma\phi_n^2+\omega+F_n)x_n+V(x_{n+1}+x_{n-1})\ . \tag{18}$$

The linear stability depends on the spectral properties of the two tridiagonal matrices A with diagonal elements $\gamma\phi_n^2+\omega+F_n$ and off-diagonal elements V and B having diagonal elements $3\gamma\phi_n^2+\omega+F_n$ and off-diagonal elements V. Linear stability requires the eigenvalues of A and B to be positive. We have shown numerically that these conditions are fulfilled for the multipulse excitation patterns considered in this paper. Finally, we remark that also the heteroclinic connection can be exploited to construct multipulse dark solitonlike excitations.

In conclusion, we have developed a method to create localized multiple pulse solutions of the nonintegrable DNLS with an external potential. To this aim we have exploited homoclinic and heteroclinic connections related with the map of the stationary problem. The merit of this method is that it enables us to control the location of the individual pulses on the lattice as well as their amplitudes.

ACKNOWLEDGMENTS

This work was supported by the Deutsche Forschungsgemeinschaft via Sonderforschungsbereich 337.

[1] J. C. Eilbeck, P. S. Lomdahl, and A. C. Scott, Physica D **16**, 318 (1985).
[2] V. M. Kenkre and D. K. Campbell, Phys. Rev. B **34**, 4959 (1986).
[3] A. S. Davydov and N. I. Kislukha, Phys. Status Solidi B **59**, 465 (1973).
[4] N. Finlayson and G. I. Stegeman, Appl. Phys. Lett. **56**, 2276 (1990).
[5] Y. Chen, A. W. Snyder, and D. J. Mitchell, Electron. Lett. **26**, 77 (1990).
[6] F. Delyon, Y.-E. Levy, and B. Souillard, Phys. Rev. Lett. **57**, 2010 (1986).
[7] M. I. Molina, W. D. Deering, and G. P. Tsironis, Physica D **66**, 135 (1993).
[8] T. Holstein, Ann. Phys. (N.Y.) **8**, 325 (1959).
[9] W. Chen and D. L. Mills, Phys. Rev. Lett. **58**, 160 (1987); D. L. Mills and S. E. Trullinger, Phys. Rev. B **36**, 947 (1987); H. G. Winful, Appl. Phys. Lett. **46**, 527 (1985).
[10] Yu.S. Kivshar, Phys. Rev. Lett. **70**, 3055 (1993).
[11] A. B. Aceves, C. De Angelis, A. R. Rubenchik, and S. K. Turytsin, Opt. Lett. **19**, 329 (1994).
[12] A. B. Aceves, C. De Angelis, S. Trillo, and S. Wabnitz, Opt. Lett. **19**, 332 (1994).
[13] A. B. Aceves, C. De Angelis, T. Peschel, R. Muschall, F. Lederer, S. Trillo, and S. Wabnitz, Phys. Rev. E **53**, 1172 (1996).
[14] Yu.S. Kivshar, Phys. Rev. E **48**, 4132 (1993).
[15] Ch. Claude, Yu.S. Kivshar, K. H. Spatschek, and O. Kluth, Phys. Rev. B **47**, 14 228 (1993).
[16] Yu.S. Kivshar and D. K. Campbell, Phys. Rev. E **48**, 3077 (1993).
[17] D. Cai, A. R. Bishop, and N. Grønbech Jensen, Phys. Rev. Lett. **72**, 591 (1994).
[18] Yu.S. Kivshar and M. Salerno, Phys. Rev. E **49**, 3543 (1994).
[19] E. W. Laedke, K. H. Spatschek, and S. K. Turitsyn, Phys. Rev. Lett. **73**, 1055 (1994).
[20] R. S. MacKay and S. Aubry, Nonlinearity **7**, 1623 (1994).
[21] D. Bambusi, Nonlinearity **9**, 433 (1996).
[22] P. Marquié, J. M. Bilbault, and M. Remoissenet, Phys. Rev. E **51**, 6127 (1995).
[23] M. J. Ablowitz and P. A. Clarkson, *Solitons, Nonlinear Evolution Equations and Inverse Scattering* (Cambridge University Press, New York, 1991).
[24] R. Scharf and A. R. Bishop, Phys. Rev. A **43**, 6535 (1991).
[25] B. M. Herbst and M. J. Ablowitz, Phys. Rev. Lett. **62**, 2065 (1989).
[26] D. Hennig, K. Ø. Rasmussen, H. Gabriel, and A. Bülow, Phys. Rev. E **54**, 5788 (1996).
[27] J. Moser, *Stable and Random Motions in Dynamical Systems* (Princeton University Press, Princeton, 1973).
[28] P. Glendinning and C. Sparrow, J. Stat. Phys. **35**, 645 (1984).
[29] A. Mielke, P. J. Holmes, and O. O'Reilly, J. Dyn. Diff. Eqns. **4**, 95 (1992).
[30] J. C. Alexander and C. K. R. T. Jones, J. Reine Angew. Math. **446**, 49 (1994).
[31] A. R. Bishop, M. G. Forest, D. W. McLaughlin, and E. A. Overmann, Phys. Lett. A **144**, 17 (1990).
[32] A. R. Bishop, R. Flesch, M. G. Forest, D. W. McLaughlin, and E. A. Overmann, SIAM (Soc. Ind. Appl. Math.) J. Math. Anal. **21**, 1511 (1990).
[33] G. Haller and S. Wiggins, Physica D **85**, 311 (1995).
[34] B. Sandstede, C. K. R. T. Jones, and J. C. Alexander, Physica D **106**, 167 (1997).
[35] R. Camassa, Physica D **84**, 357 (1995).
[36] V. V. Konotop, O. A. Chubykalo, and L. Vázquez, Phys. Rev. E **48**, 563 (1993).
[37] D. Cai, A. R. Bishop, N. Grønbech-Jensen, and M. Salerno, Phys. Rev. Lett. **74**, 1186 (1995); D. Cai, A. R. Bishop, and N. Grønbech Jensen, Phys. Rev. E **52**, 5784 (1995); **53**, 1202 (1996).
[38] J. Coste and J. Peyrard, Phys. Rev. B **39**, 13 086 (1989).
[39] Yi Wan and C. M. Soukoulis, Phys. Rev. A **41**, 800 (1990); in *Disorder and Nonlinearity*, edited by A. R. Bishop, D. K. Campbell, and S. Pnevmatikos (Springer, Berlin, 1989), pp. 27–37.
[40] J. B. Page, Phys. Rev. B **41**, 7835 (1990).
[41] A. J. Sievers and S. Takeno, Phys. Rev. Lett. **61**, 970 (1988).